

Nikolay RUZHENTSEV¹, Oleg GRIBSKY², Sergey MALTSEV², Sergey SHEVCHUK², Vladimir PAVLIKOV¹, Gleb CHEREPNIN¹, Simeon ZHYLA¹, Eduard TSERNE¹

¹ National Aerospace University "Kharkiv Aviation Institute", Kharkiv, Ukraine

² State Enterprise "Research Institute "Orion", Kyiv, Ukraine

ACTIVE-PASSIVE PULSE NOISE RADAR OF THE 3MM RANGE AND THE RESULTS OF PRELIMINARY TESTS

The **subject** of this manuscript is broadband noise signals and systems. The **aim** of this research is to show the results of a modern active-passive 3-mm waveband system consisting of a noise-pulsed radar and a radiometer. Noise radar systems (NRS) based on broadband signals are characterized by high resolution, accuracy, and information content when performing unambiguous measurements of the range and speed of targets, as well as increased electromagnetic compatibility and noise immunity. These distinctive features of NRS determine the relevance of their construction for practical tasks of short- and medium-range radar. Additional opportunities for ensuring secrecy, reliability of detection of objects, and their tracking are provided by the combination of active and passive location modes in conjunction with advancement to the short-wave part of the millimeter (MM) wave band (WB). The most important characteristic of any pulsed radar, which largely determines its potential for practical application, is the operating frequency, as well as the shape and width of the probing signal spectrum. The main **idea** of this work is to describe the construction scheme and the results of preliminary tests of the developed active-passive system in the 94 GHz band with a noisy 20–100 ns illumination pulse in the 5 GHz band. The obtained values of the energy potential of the system in the active location mode (-105 dB) and the achieved radiometer sensitivities in the passive mode (0.007K and 0.03K) make it possible to observe ground and air objects at a distance of several kilometres. Noted that the measured parameters of the radar, in the case of processing the received signal by pulse compression methods, make it possible to count on ensuring the resolution of targets in range at the level of 10–15 cm. A multiple (more than an order of magnitude) decrease in the interference fluctuations of the received signal, which is due to the facet nature of the backscattering of targets, has experimentally demonstrated using a noise probing pulse compared to a single-frequency pulse. The methods for further work on the development and practical application of the constructed measuring system are outlined.

Keywords: noise radar; active-passive systems; broadband noise signals; millimetre range; radiometers.

1. Introduction

Motivation. All modern users of radar systems are in constant need of improving the quality and quantity of information from the observed space. The most important components for meeting such needs are the following: increasing the angular resolution and range resolution of radars, reducing spatio-temporal fluctuations of the received signal, and ensuring the secrecy of monitoring the radar situation.

Promising radar systems should provide improved target recognition by constructing long-range portraits, increasing the accuracy of determining the speed and coordinates of objects, and reducing the likelihood of missing targets and false alarms. The solution of these complex problems in modern radar systems can be achieved using efficient broadband technologies [1, 2] and new solutions in the field of signal processing [3, 4].

State of the Art. Active and passive noise locations are promising areas of research to solve this problem. In

this regard, in recent years, interest in noise radar methods has increased [5].

Noise radar systems based on broadband signals are characterized by high resolution [7, 8], accuracy and information content [9, 10] when performing unambiguous measurements of the range, speed [11, 12] and angular coordinates of targets [13, 14]. They are also characterized by electromagnetic compatibility and noise immunity with respect to external and harmful interference, for example, with facet scattering or multipath propagation of signals. Devices in these studies currently involve the use of narrowband deterministic signals, which limits their potential technical characteristics. Given the significant breakthrough in the development of wideband and ultra-wideband radio electronics, it is promising to create on-board radio complexes capable of obtaining the necessary information using wideband stochastic signals.

Noise radars are also distinguished by the secrecy of their emissions and the low probability of detection by radio equipment. An important characteristic of such ra-

dars is their electromagnetic compatibility with other radio equipment because of the low spectral density of broadband probing signals. These distinctive features of NRS determine the relevance of their construction for various practical applications of short [15, 16] and medium-range radar with ultrahigh resolution [17, 18]. These papers describe the concept of cognitive radar and the problem of corrupted radar super-resolution, which is a generalization of compressed radar super-resolution in which one aims to recover the continuous-valued delay-Doppler pairs of moving objects from a collection of corrupted and noisy measurements. This novel-compressed sensing approach offers great potential for better resolution than that of classical radar.

Additional improvements in the secrecy of operation and an increase in the target detection range can provide spatial separation of the receiving and transmitting radar units. For example, in work [5], the authors established mathematical similarities between noise radar and dual-channel synthetic aperture radar and proposed a simplified evaluation system that results in identical detection performance in the simulation. In this study, spatial separation of the radar transmitter and receiver units is considered as a means of reducing the masking effect in noise radars [6]. The system uses pseudo-random noise, which is generated digitally at the receiver and transmitter units. This study shows that by separating the transmitter and receiver unit, the masking effect is reduced significantly compared with a monostatic setup. This reduction is sufficient for the system to detect a slow-flying UAV. However, the complexity of digitalization in the MM wavelength and the short-wave part of the centimeter WB has so far limited the scope of application of this approach.

Additional opportunities for ensuring stealth and reliability of object detection and tracking are provided by combining passive [19, 20] and active [21, 22] location modes in conjunction with advancement to the short-wavelength part of the MM wave band. Advancement into this range increases the radar cross-section (RCS) and contrasts of the observed objects while improving the spatial resolution of the radar.

In our works [23, 24], based on the developed mathematical apparatus and computer modeling, we demonstrated the possibility of detecting aircraft in passive radiometry mode at ranges reaching several kilometers, which was then experimentally confirmed using a specially developed four-frequency radiometric complex. The works [23, 24] describe the possibilities of increasing the probability of target detection in ultra-wideband location modes by calculation.

This work is a continuation of works [23, 24] and is devoted to the description of a combined active-passive system in the 3 mm WB and preliminary results of testing

its performance. The described active-passive system, consisting of a noise pulse radar and a radiometer, was developed and manufactured at the Department of Aerospace Radio-Electronic Systems of National Aerospace University "Kharkiv Aviation Institute".

Objectives. The purpose of this study is to describe the developed design, construction schemes, and parameters of key elements of an active-passive noise radar of the 3 mm WB, as well as to present the results of its preliminary field tests.

The described system, characterized by high stealth and potentially increased range resolution, is intended for subsequent research and comparison of radar and radiometric contrasts of UAVs, knowledge of which is necessary to detect aircraft located against the background of the Earth's surface or sky.

To achieve the stated goals of the work, it was necessary to solve and complete tasks such as developing a scheme for constructing single-antenna and dual-antenna versions of the radar (section 2), ensuring the configuration and measurement of the parameters of its key elements and the assembled system (section 3), working out issues of a methodological nature (section 4), conducting a cycle of full-scale tests of the radar's performance, and outlining ways for further development of this promising area of work (section 5).

2. Scheme of construction and main parameters of the impulse noise radar

The most important characteristic of any pulsed radar, which largely determines its potential for practical application, is the operating frequency, as well as the shape and width of the probing signal spectrum. In the designed radar, the average operating frequency is 94 GHz, which is located near the central part of the atmospheric transparency window.

It is known [25] that because of the involvement of received signal processing procedures by pulse compression methods, the expansion of the frequency band of the pulse itself makes it possible to achieve multiple increases in resolution, in both the range and speed of observed objects. In practice, this procedure can be implemented in two ways: by fast, almost linear, frequency tuning within a pulse or by using a stochastic generator, in which rapid random changes in the generation frequency occur, which turns its spectrum into a noise-like one. Both of these approaches for bandwidth expansion in one pulse are difficult to implement, even with the use of digital signal synthesis, because they require an instantaneous bandwidth of more than 3 GHz. However, such a signal can be formed parametrically because of the properties of the active element of the transmitter.

One of these options is the behavior of pulsed impact ionization avalanche transit-time (IMPATT) diodes when they are included in low-Q resonators, which makes it possible to achieve a change in the generation frequency within a 100-ns pulse in GHz. To build a noise radar, this type of generator is used. The transmitter is built based on a pulse generator with IMPATT diode and is capable of generating pulses with a duration of 20, 30, and 100 ns at a 50% power level at a pulsed power level of 1 W in the 5 GHz band with a center frequency of 94 GHz.

Figure 1 shows a scheme for constructing a radar with noise filling of the probing pulse. The RF element base used in its construction and some circuit solutions are based on the developments of the State Enterprise "Research Institute "Orion".

The radar works as follows. The transmitter signal through the transmit-receive circulator enters a two-mirror Cassegrain antenna system (AS) with an aperture of 15 cm (radiation pattern width (RP) is 2.1°). The receiver with a two-band operation mode in the 2 GHz band was built according to a superheterodyne scheme.

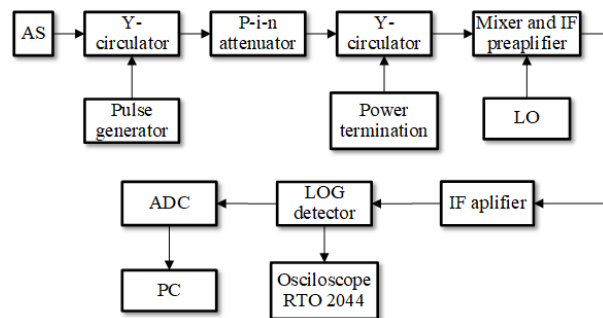


Fig. 1. Block diagram of the noise pulse radar of the active-passive measuring system 3 MM WB

The signal reflected by the target, having passed the receive-transmit circulator, the p-i-n attenuator, and the decoupling Y-circulator, enters the balanced mixer. The receiver uses a high-speed p-i-n diode modulator-attenuator with a switching time of no more than 2 ns. The modulator closes when the transmitter is in operation to prevent the receiver from being damaged. A balanced feed-through mixer with an intermediate frequency (IF) low-noise amplifier (LNA) structurally built into its housing provides a single-sideband noise figure of 6 dB at frequencies of 94 ± 1.5 GHz. The local oscillator (LO) signal, based on the Gunn diode, is tuned to a frequency of 94 GHz and is fed to the mixer from the rear side of the mixing chamber feed-through waveguide.

After amplification in the LNA and IF, the intermediate frequency signal is fed to a logarithmic envelope detector with a bandwidth of 40 MHz. The sensitivity of

the logarithmic detector is 12 mV/dB. The pulse generator synchronizes all radar operations. The accumulation and registration of the received signal is performed using the service capabilities of a Rohde-Schwarz (RTO 2044) 5 GHz digital oscilloscope or an ADC-PC circuit. The measured value of the dynamic range of the receiver exceeds 60 dB. The appearance of the microwave part of the noise-incoherent pulsed radar is shown in Fig. 2.

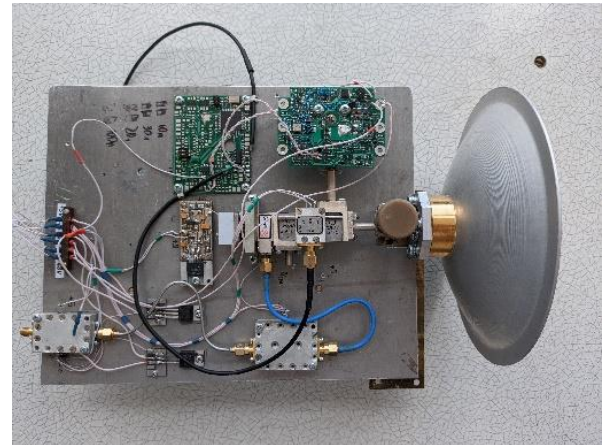


Fig. 2. Appearance of the high frequency (HF) part of the noise incoherent pulse radar 3 MM WB

3. Results of the preliminary tests of the noise impulse radar

Preliminary full-scale tests of the built active-passive system carried out at KhAI demonstrate that in the active radar mode for weakly reflecting objects that were observed at distances up to 2 km (without using special methods for processing the received signal), a range resolution of approximately 3 m was obtained with a pulse duration of 20 ns. At the same time, the minimum target detection range from the transceiver antenna was approximately 2 m. The transmitter used in this radar with a noisy pulse in the 5 GHz band, as well as the receiver band matched with it, will in the future make it possible to increase the range resolution to a few centimeters by involving the procedures for processing the received signal by pulse compression methods.

Figure 3 and Figure 4, as examples, show oscillograms of the radar output signals observed on the oscilloscope screen during trial sounding of the surrounding space at short and medium ranges, respectively.

It is appropriate to note that in addition to the potential possibility of multiple improvements in the resolution of the developed radar, another advantage of using a noise probing signal, compared to a monofrequency signal, should be considered a multiple reduction in the interference fluctuations of the received signal, which are

caused by the facet nature of the back reflection from most of the observed types of targets. Therefore, in the case of using a probing signal in the form of a noise-like pulse, the movement of one of the 2 corner reflectors relative to the other in the spot of the antenna pattern led to 1–2 dB changes in the total RCS.

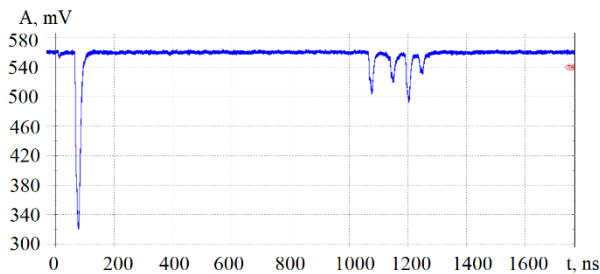


Fig. 3. The received signal 20ns reflected from the windows of a building with four air conditioners in the spot of the antenna pattern at an angle of 45° at a distance of 180 m (a four-component pulse on the right). On the left, the suppressed transmitter pulse leaked into the receiver

When conducting a similar experiment using a monofrequency pulse transmitter, a significant, up to 15 dB, change in the total RCS was determined. This result makes it possible to count on the appearance of additional possibilities for selecting targets according to the characteristic value of their RCS when using a noise-like probing pulse.

4. Main parameters of noise radar during transition to passive (radiometric) location mode

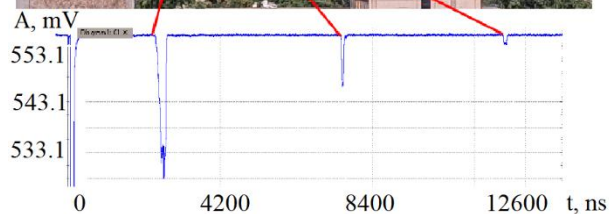
The HF part of the noise-filled impulse radar circuit described in the previous section was integrated into the radiometer circuit. The practical implementation of this technical solution does not require significant changes to the HF part of the radar, except installing a Y-circulator as an isolator between the protective modulator and the mixer. The same structure and spectral characteristics in the operating frequency band of the receiver, the transmitter signal, and the equilibrium radiation emitted by environmental objects make it possible to use the microwave part of one receiver both for radiometry and for active location by spreading their work in time.

At the same time, to build a radiometer based on the HF path of the noise radar, it was also necessary to replace part of the IF path (after the intermediate frequency preamplifier of radar) with an IF with a gain of 27 dB in the 0.2–2.3 GHz band and a square-law detector at the output. The need for such a replacement was due to the

fact that the use of a logarithmic detector at the output of the IF channel of the NRS makes it difficult to calibrate the radiometer using the 2-load method (there is a deterioration in accuracy due to the nonlinearity of K_{signal} propagation in the logarithmic radar detector).



a)



b)

Fig. 4. Experimental conditions (a) where red spot is the approximate position of the RP and the received signal (b) is reflected from three buildings at a distance of 1.8 km (right impulse) and 1.14 km (middle impulse) and 0.39 km (left impulse). On the left, the transmitter pulse leaked into the receiver.

Figure 5 shows a schematic of the construction of the developed 3-mm radiometer as part of a noise-pulsed radar. In the process of building a radiometer combined with a single-antenna version of the NRS, it was necessary to abandon the scheme of the total power radiometer with an HF LNA at the input in favor of a modulation scheme without an HF LNA. Such a replacement is nec-

essary to compensate for the instability of K signal transmission in the HF and IF paths of the radar receiver and because of the critical dependence of the HF LNA on high transmitter power levels leaking into the receiver. In the implemented modulation scheme for constructing the radiometer, the alternate switching of the noise signal coming from the antenna and from the blocking attenuator is provided by a 1000 Hz meander, which was simultaneously supplied from the synchronizer to the ADC for digital synchronous detection and to the p-i-n attenuator, intended in active location mode to block the receiver from the transmitter pulse leaking through the Y-circulator. Together, these measures made it possible to increase the fluctuation sensitivity of the radiometer in the modulation design by almost two orders of magnitude compared to a radiometer built on a similar element base according to the full power scheme.

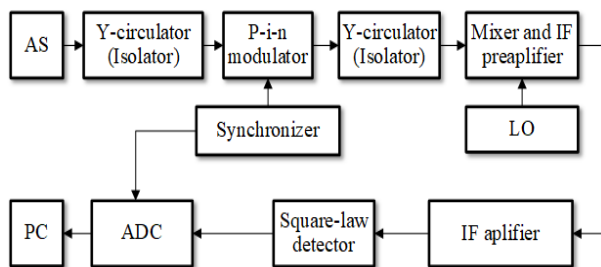


Fig. 5. Scheme of a radiometer as part of a noise-pulsed radar

This sensitivity of the system makes it possible to detect flying objects observed against the background of the sky [24, 29] at distances of up to several kilometers.

Figure 6 shows fragments of the calibration records obtained by determining the sensitivity of the constructed radiometer using the two-load method. Here, as matched loads, the radiation of the “Vors”-type radio-absorbing material received by the antenna ($T_o=298K$) and the radiation of the near-zenith region of a clear atmosphere are used. The radio-brightness temperature of the atmosphere was calculated using the Liebe radiophysical model [26] and the meteorological model of the altitude distribution of meteorological parameters ERA-15 [27, 28] based on measured surface meteorological data. The measured fluctuation sensitivity is approximately 0.03 K with an integration time of 1 s.

Radiometer in a two-antenna version of an active-passive system

There are two ways to provide simultaneous mode of active noise and passive location (operating mode without turning off the transmitter and sequential switching of the IF and LF parts of the receiver). One of them

is based on the use of an additional second antenna with a radiometric receiver. The second method can be implemented based on the already described single-antenna variant by providing the combination of active and passive modes by the method of their separation within the inter-pulse interval of the radar (in this radar – 50 μ s). The implementation of the second, single-antenna variant of combining an active-passive noise radar with the separation of these modes within the inter-pulse interval of the radar is supposed to be implemented in the subsequent stages of this research.

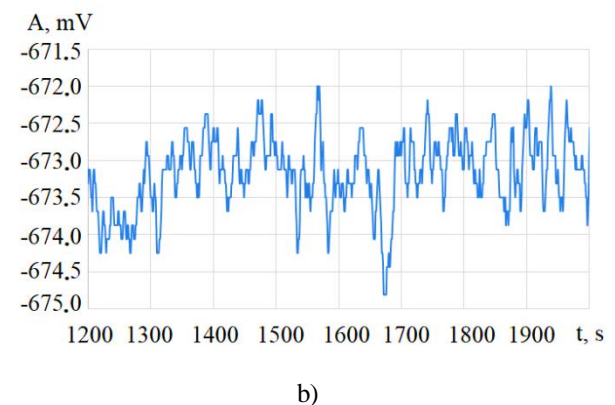
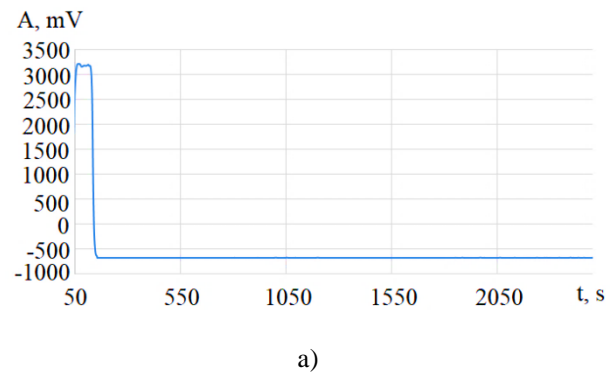


Fig.6 Fragments of recording the output level of the signal (mV) received from the matched load (ML) of the antenna (298K) and the signal received from the clear sky toward 40° from the zenith (79 K) during the calibration of the radiometer (a), as well as an enlarged fragment of the recording of the output signal of the antenna received from ML (b)

At the current stage of work, the first option has been developed and implemented using a second antenna with a separate radiometer. Its drawback, which consists of the need to use an additional antenna system, is to some extent compensated by an increase in the range of the passive system due to additional possibilities for the implementation of a radiometer that is many times more sensitive. The use of a stand-alone radiometer HF path,

not connected to the radar circuit, makes it possible to increase its sensitivity due to its broadband operation mode, as well as due to the use of HF LNA in the input circuits of the device and the use of a direct amplification circuit.

Receiving systems for radiometers are usually built using direct amplification circuits or superheterodyne circuits, i.e., full power circuits or modulation circuits. Direct amplification schemes provide a large bandwidth and no conversion losses in the mixer, and hence increased sensitivity, which is especially important in passive radar applications.

Although the potentially achievable sensitivity of total power radiometers is twice as good as that of modulation-type radiometers, modulation-type radiometers have found the widest application in the short millimeter wave range until recently. Such schemes make it possible to compensate for the negative effect of path gain instability on radiometer sensitivity. Based on the above considerations, its construction requires a direct amplification circuit of the modulation type.

In the process of designing and building modern radiometers, it also makes sense to pay attention to the latest achievements in the field of circuitry and technological solutions of radio electronics, which are based on the use of GaAs technologies and have made it possible to create ultra-low-noise transistor amplifiers with noise temperatures of only a few hundred K up to 3mm WB. Therefore, it is advisable to use the LNA by placing it in the input circuits of any radiometer circuit.

Figure 7 shows a schematic of the construction of a 3-mm range radiometer connected to a separate antenna of the measuring system, and Figure 8 shows the external view of the RF path of this radiometer.

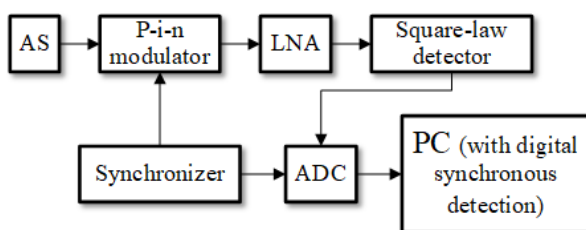


Fig. 7 Scheme of a radiometer as a part of a two-antenna variant of an active-passive radar

The main parameters of the nodes of the HF part of the radiometer built according to this scheme, which determine its main parameter, the fluctuation sensitivity, are as follows:

- signal loss in the p-i-n modulator in the band 75-110 GHz does not exceed 0.4 dB;
- the noise figure of the LNA in the band 75-110 GHz does not exceed 3dB;
- the sensitivity of the square-law detector in the band 75-110 GHz is not worse than 750 mV/W.

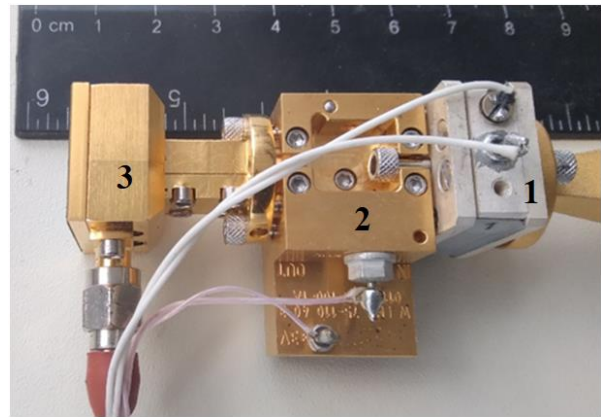


Fig. 8. External view of the HF part of the radiometer in the range of 75-110 GHz built at the Department of Aerospace Radioelectronic Systems of KhAI:
1 – p-i-n modulator, – LNA 75-110 GHz,
3 – square-law detector

The procedure for processing the received signal is performed by its synchronous detection and accumulation of the signal in digital form after the ADC is connected to the square-law detector.

Figure 9 shows the calibration records of this radiometer in the modulation mode, which were obtained when estimating its fluctuation sensitivity by the two-load method, according to the procedure already described for the radiometer built into the single-antenna version of the system. To estimate the dispersion of measurements, filters and methods similar to those used in image filtering [30, 31] can be applied.

Measured values of fluctuation sensitivity with an integration time of 1 s in the absence of cooling of the receiver with a reception band of 75-110 GHz (at room temperature) amounted to approximately 0.007 K.

This sensitivity value allows, for example, further double the detection range of flying objects compared with the radiometer described in the previous section. It is appropriate to note that an attempt to implement the described radiometer in the full power mode on this element base showed the sensitivity value by almost two orders of magnitude worse – its value is about 0.6 K.

5. Discussion

The developed scheme for constructing a radar (Section 2) and the parameters achieved during its implementation (energy potential, receiver sensitivity, dynamic range and spectral width of the sounding signal) make it possible to provide a practical solution to various problems of active location in the range from 2m to several kilometers (Section 3) with a range resolution of 2m to 15m (depending on the pulse duration set within 20–100 ns).

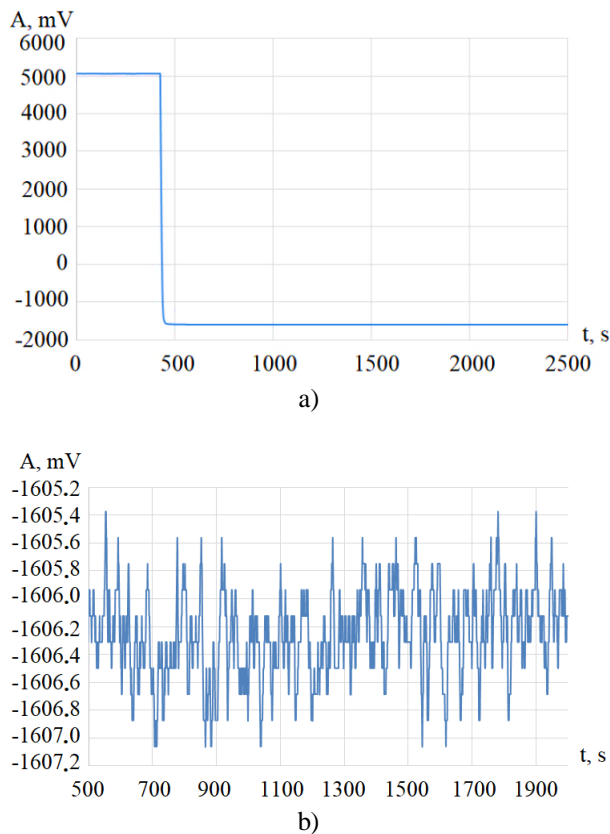


Fig. 9. Fragments of recording the output level of the signal (mV) from the matched load of the antenna (290K) and the signal from the sky in the direction of 60° from the zenith (126K) during calibration of the radiometer (a) and an enlarged fragment of the recording from the ML of the antenna (b)

This result can be considered acceptable for solving many short-range problems. It is also appropriate to note that the spectral width, operating frequency range, and emitted power level implemented in the active location mode provide not only a significant increase in the stealth of the developed system but also can significantly increase the range resolution (by more than an order of magnitude) when using the received data processing signal using the pulse compression method. In the near future, achieving a range resolution of 10–20 cm with repeated minimization of the faceted nature of fluctuations of the received signal will allow to count on solving the urgent problem of constructing radar portraits of many types of targets to ensure their identification.

The highly sensitive receiver circuit implemented in the radar is designed considering the possibility of its use in the passive location mode (Section 4). Simultaneously, laboratory studies of sensitivity showed the need to switch the radiometer to modulation mode to eliminate the influence of insufficient stability of the overall gain of the path to achieve a high sensitivity of 0.03 K. A similar approach was used in the development of an ultra-

wideband 3mm radiometer in a two-antenna version of the active-passive system (section 4.1). Technical solutions such as the choice of a direct amplification modulation scheme, the use of a low-noise LNA at the input, and a 35 GHz receiving band made it possible to improve the sensitivity achieved in the single-antenna version of the system by 4 times.

The use of a combined active-passive mode allows not only to further increase the secrecy of the system but also increases the likelihood of detecting low-contrast objects observed against the background of the sky or the Earth's surface. To specify and evaluate the advantages of using such combined active-passive algorithms and observation modes, it is necessary to perform additional full-scale and computational studies of this issue that we have planned using the measuring complex described in this work.

Conclusions

The developed, built, and experimentally tested active-passive pulsed noise radar of the 3 mm WB demonstrated its performance during field tests at distances from a few meters to several kilometers. The pulse radar and radiometer device described herein includes units that are built on the basis of a modern element base with the given measured parameters and are at the level of the latest achievements in the small-scale field of electronic technology.

Calculation estimates and preliminary experiments also show that the obtained values of the radar energy potential, the spectrum widths of the emitted noise pulse and the received signal of thermal noise or illumination noise, as well as the achieved sensitivity values of radiometers, make it possible to ensure high-precision and comprehensive studies aimed at optimizing the use of promising active-passive modes in target detection and tracking tasks.

The work also notes the expediency of developing and using pulse compression methods in the described measuring complex by correlative processing of the received signal to increase the spatial resolution in range multiple times (by more than an order of magnitude). The use of this opportunity should make it possible to recognize and identify observed objects by constructing their radar portraits.

Future research directions. Further development of the described measuring system will be aimed at the implementation of single-antenna parallel active and passive location modes by separating them within the interpulse interval. There are also plans to develop software and methodological support for the digital processing of received signals by pulse compression.

Successful solution of these problems will enable the formation of a radar portrait of an object and the

development of systems for automatic recognition of an object by its portrait, which qualitatively increases the information capabilities of traditional radar systems.

Radars built using the proposed technology can be used in navigation [32, 33], remote sensing [34, 35], and cognitive radar cells [35, 36].

Contribution of authors: conceptualization – **Simeon Zhyla, Vladimir Pavlikov, Oleg Gribsky**; methodology – **Oleg Gribsky, Vladimir Pavlikov**; simulation – **Simeon Zhyla, Eduard Tserne**; conducting the experiment – **Nikolay Ruzhentsev, Gleb Cherepnin**; validation – **Vladimir Pavlikov**; formal analysis – **Simeon Zhyla, Oleg Gribsky**; investigation – **Nikolay Ruzhentsev**; resources – **Sergey Maltsev**; data curation – **Sergey Shevchuk**; writing- original draft – **Nikolay Ruzhentsev, Sergey Maltsev**; writing-review and editing – **Nikolay Ruzhentsev, Gleb Cherepnin, Sergey Maltsev**; supervision – **Sergey Shevchuk**; project administration – **Nikolay Ruzhentsev**; funding acquisition – **Simeon Zhyla, Vladimir Pavlikov**.

All authors have read and agreed to the published version of this manuscript.

Acknowledgement. The Ministry of Education and Science of Ukraine funded this work. The state registration number of the project «*Design, development of a layout and experimental study of a passive radar with a noise-immune target illumination signal for detecting UAVs*» is No. 0123U102000.

References

1. Oloumi, D., Winter, R. S. C., Kordzadeh, A., Boulanger, P., & Rambabu, K. Microwave imaging of breast tumor using time-domain UWB circular-SAR technique. *IEEE transactions on medical imaging*, 2020, vol. 39, no. 4, pp. 934-943. DOI: 10.1109/TMI.2019.2937762.
2. Schantz, H. *The art and science of ultrawideband antennas*. Boston, Artech House Publ., 2015. 563 p.
3. Oloumi, D. *Ultra-wideband synthetic aperture radar imaging: Theory and applications*. Edmonton, Department of Electrical and Computer Engineering University of Alberta, 2016. 179 p.
4. Hunziker, P., Morozov, O. V., Volosyuk, O. V., Volosyuk, V. K., & Zhyla, S. S. Improved method of optical coherence tomography imaging. *2016 IEEE International conference on mathematical methods in electromagnetic theory (IEEE MMET-2016)*, 2016, pp. 421-424. DOI: 10.1109/MMET.2016.7544109.
5. Luong, D., Balaji, B., & Rajan, S. A closed-form estimate for the correlation coefficient of noise-type radars. *2022 IEEE Radar Conference (RadarConf22)*, 2022, pp. 1-5. DOI: 10.1109/RadarConf2248738.2022.9764192.
6. Ankel, M., Jonsson, R., Bryllert, T., Ulander, L. M. H., & Delsing, P. Bistatic noise radar: Demonstration of correlation noise suppression. *IET Radar, Sonar and Navigation*, 2023, vol. 17, iss. 3, pp. 351-361. DOI: 10.1049/rsn2.12345.
7. Feghhi, R., Oloumi, D., & Rambabu, K. Design and development of an inexpensive sub-nanosecond gaussian pulse transmitter. *IEEE transactions on microwave theory and techniques*, 2019, vol. 67, no. 9, pp. 3773-3782. DOI: 10.1109/TMTT.2019.2918298.
8. Pavlikov, V., Volosyuk, V., Shmatko, O., Zhyla, S., Tserne, E., & Dyomin, A. Signal processing algorithm for noise noncoherent wideband helicopter altitude radar. *2022 IEEE 16th international conference on advanced trends in radioelectronics, telecommunications and computer engineering (TCSET-2022)*, 2022, pp. 457-461. DOI: 10.1109/TCSET55632.2022.9767086.
9. Bräunlich, N., Wagner, C. W., Sachs, J., & Galdo, G. D. Configurable Pseudo Noise. Radar Imaging System Enabling Synchronous MIMO Channel Extension. *Sensors*, 2023, vol. 23, iss. 5, article no. 2454. DOI: 10.3390/s23052454.
10. Narayanan, R. M. Noise Radar Techniques and Progress. *Chapter 9 in Advanced Ultrawideband Radar: Signals, Targets, and Applications*. Boca Raton: CRC Press, 2016, pp. 323-361. DOI: 10.1201/9781315374130-10.
11. Kim, E., Kim, I., Han, S., Lee, J., & Shin, S. A Wideband Noise Radar System Using a Phased Array with True Time Delay. *Remote Sens*, 2022, vol. 14, iss. 18, article no. 4489. DOI: 10.3390/rs14184489.
12. Chapursky, V. V., Sablin, V. N., Kalinin, V., & Vasilyev, I. A. Wideband random noise short range radar with correlation processing for detection of slow moving objects behind the obstacles. *Tenth International Conference on Ground Penetrating Radar (GPR 2004)*, 2004, pp. 199-202. DOI: 10.1109/ICGPR.2004.179955.
13. Ilchenko, M. E., Kalinin, V. I., Narytnyk, T. M., & Didkovski, R. M. Potential performance of the communication systems using autocorrelation reception of shift-keyed noise signals. *Telecommunications and radio engineering*, 2014, vol. 73, iss. 11, pp. 955-976. DOI: 10.1615/TelecomRadEng.v73.i11.20.
14. Kalinin, V., Panas, A., Kolesov, V., & Lyubchenko, V. Ultrawideband wireless communication on the base of noise technology. *2006 International conference on microwaves, radar & wireless communications. (MIKON 2006)*, 2006, pp. 615-618. DOI: 10.1109/MIKON.2006.4345254.
15. Shin, H. J., Narayanan, R. M., & Rangaswamy, M. Ultrawideband noise radar imaging of impenetrable cylindrical objects using diffraction tomography. *International journal of microwave science and technology*, 2014, vol. 2014, pp. 1-22. DOI: 10.1155/2014/601659.

16. Herman, M. A., & Strohmer, T. High-Resolution radar via compressed sensing. *IEEE transactions on signal processing*, 2009, vol. 57, no. 6, pp. 2275–2284. DOI: 10.1109/TSP.2009.2014277.
17. Zhyla, S., Volosyuk, V., Pavlikov, V., Vlasenko, D., Borodavka, V., & Pidlisnyi, O. Structural diagram of an aerospace cognitive radar for the earth remote sensing. *2022 12th International conference on dependable systems, services and technologies. (DESSERT-2022)*, 2022, pp. 1-6. DOI: 10.1109/DESSERT58054.2022.10018767.
18. Bayat, S., & Daei, S. Separating radar signals from impulsive noise using atomic norm minimization. *IEEE Transactions on Circuits and Systems II: Express Briefs*, 2021, vol. 68, no. 6, pp. 2212-2216. DOI: 10.1109/TCSII.2020.3045226.
19. Ruzhentsev, N., Zhyla, S., Pavlikov, V., Volosyuk, V., Cherepnin, G., & Kosharskyi, V. UAV radio thermal contrasts in MM and CM wavelength ranges. *2022 IEEE 2nd Ukrainian microwave week. (UKRMW-2022)*, 2022, pp. 711-715. DOI: 10.1109/UkrMW58013.2022.10037002.
20. Ruzhentsev, N., et al. Radio-Heat contrasts of UAVs and their weather variability at 12 GHz, 20 GHz, 34 GHz, and 94 GHz frequencies. *ECTI transactions on electrical engineering, electronics, and communications*, 2022, vol. 20, no. 2, pp. 163–173. DOI: 10.37936/ecti-ec.2022202.246878.
21. Pavlikov, V., Volosyuk, V., Zhyla, S., Tserne, E., Shmatko, O., & Sobkolov, A. Active-Passive radar for radar imaging from aerospace carriers. *19th International conference on smart technologies (IEEE EUROCON 2021)*, 2021, pp. 18-24. DOI: 10.1109/EUROCON52738.2021.9535619.
22. Pavlikov, V., et al. Radar imaging complex with SAR and ASR for aerospace vehicle. *Radioelectronic and computer systems*, 2021, no. 3, pp. 63–78. DOI: 10.32620/reks.2021.3.06.
23. Ruzhentsev, N., et al. Block diagram of a multi-frequency radiometric complex for UAV detection in different meteorological conditions. *Information and telecommunication sciences*, 2021, no. 2, pp. 50–57. DOI: 10.20535/2411-2976.22021.50-57
24. Ruzhentsev, N., Zhyla, S., Pavlikov, V., Cherepnin, G., Tserne, E., & Kosharskyi, V. Theoretical bases of multi frequency radiometric systems development for UAV detection against the background of atmospheric radiation. *2022 IEEE 16th International conference on advanced trends in radioelectronics, telecommunications and computer engineering (TCSET-2022)*, 2022, pp. 20–24. DOI: 10.1109/TCSET55632.2022.9766843
25. Volosyuk, V. K., & Kravchenko, V. F. *Statisticheskaya teoriya radiotekhnicheskikh sistem distantsionnogo zondirovaniya i radiolokatsii* [Statistical Theory of Radio-Engineering Systems of Remote Sensing and Radar]. Moscow, Fizmatlit Publ., 2008. 704 p.
26. Liebe, H. J. MPM-An atmospheric millimeter-wave propagation model. *International journal of infrared and millimeter waves*, 1989, vol. 10, no. 6, pp. 631–650. DOI: 10.1007/BF01009565.
27. Martellucci, A., Rastburg, B.A., Poiaries Baptista, J. P. V., & Blarzino, G. New reference standard atmospheres based on numerical weather products. *Abstracts of International Workshop (ClimDiff)*, 2003, clim. 1.
28. Riva, C., Martellucci, A., Kubista, E., Chonhuber, M., & Luini, L. ERA-15 climatological databases for propagation modeling. *Proc. of International Conf. (ClimDiff '05)*, 2005, pp. 12.1-12.7.
29. Xu, X., Narayanan, R. M. Impact of different correlation receiving techniques on the imaging performance of UWB random noise radar. *2003 IEEE international geoscience and remote sensing symposium (IGARSS 2003)*, 2003, pp. 4525–4527. DOI: 10.1109/IGARSS.2003.1295568.
30. Uss, M., et al. Image informative maps for estimating noise standard deviation and texture parameters. *EURASIP journal on advances in signal processing*, 2011, vol. 2011, no. 1, article no. 806516. DOI: 10.1155/2011/806516.
31. Lukin, V. V. Methods and automatic procedures for processing images based on blind evaluation of noise type and characteristics. *Journal of applied remote sensing*, 2011, vol. 5, no. 1, article no. 053502. DOI: 10.1117/1.3539768.
32. Ponomarenko, N. N., Lukin, V. V., Egiazarian, K. O., & Astola, J. T. A method for blind estimation of spatially correlated noise characteristics. *IS&T/SPIE Electronic imaging*, 2010. DOI: 10.1117/12.847986.
33. Ostroumov, I., et al. Modelling and simulation of DME navigation global service volume. *Advances in space research*, 2021, vol. 68, no. 8, pp. 3495–3507. DOI: 10.1016/j.asr.2021.06.027.
34. Pavlikov, V., Volosyuk, V., Tserne, E., Sydorenko, N., Prokofiev, I., & Peretiatko, M. Radar for aircraft motion vector components measurement. *2022 IEEE 2nd Ukrainian microwave week (UKRMW-2022)*, 2022, pp. 567-572. DOI: 10.1109/UkrMW58013.2022.10036953.
35. Zhyla, S., Volosyuk, V., Pavlikov, V., Vlasenko, D., Borodavka, V., & Pidlisnyi, O. Structural diagram of an aerospace cognitive radar for the earth remote sensing. *2022 12th international conference on dependable systems, services and technologies (DESSERT-2022)*, 2022, pp. 1-6. DOI: 10.1109/DESSERT58054.2022.10018767.
36. Guerci, J. R. *Cognitive radar: the knowledge-aided fully adaptive approach*. Boston, Artech House, 2010. 175 p.

Received 07.07.2023, Accepted 20.09.2023

АКТИВНО-ПАСИВНИЙ ІМПУЛЬСНО-ШУМОВИЙ РАДАР ДІАПАЗОНУ 3ММ ТА РЕЗУЛЬТАТИ ЙОГО ПОПЕРЕДНІХ ВИПРОБУВАНЬ

*Микола Руженцев, Олег Грибський, Сергій Мальцев, Сергій Шевчук,
Володимир Павліков, Гліб Черепнін,
Семен Жила, Едуард Церне*

Предметом дослідження є широкосмугові шумові сигнали та системи. Мета дослідження – показати результати роботи сучасної активно-пасивної системи 3 мм діапазону хвиль, що складається з шумового імпульсного радара та радіометра. Шумові радіолокаційні системи (ШРЛ) на основі широкосмугових сигналів характеризуються високою роздільною здатністю, точністю та інформативністю при виконанні однозначних вимірювань дальності та швидкості цілей, а також підвищеною електромагнітною сумісністю та завадозахищеністю. Ці відмінні особливості ШРЛ зумовлюють актуальність їх конструкції для практичних завдань РЛС малої та середньої дальності. Додаткові можливості для забезпечення скритності, надійності виявлення об'єктів і їх супроводу надає поєднання активного і пасивного режимів локації в поєднанні з просуванням на короткохвильову частину міліметрового (ММ) діапазону хвиль (ДХ). Найважливішою характеристикою будь-якого імпульсного радіолокатора, яка багато в чому визначає можливості його практичного застосування, є робоча частота, а також форма і ширина спектра зонduючого сигналу. Основною ідеєю роботи є опис схеми конструкції та результатів попередніх випробувань розробленої активно-пасивної системи в діапазоні 94 ГГц з шумовим імпульсом підсвічування 20–100 нс в діапазоні 5 ГГц. Показано, що отримані значення енергетичного потенціалу системи в режимі активної локації (-105 дБ) і досягнуті чутливості радіометра в пасивному режимі (0,007К та 0,03К) дозволяють спостерігати наземні та повітряні об'єкти на відстань у кілька кілометрів. Зазначається, що виміряні параметри РЛС, у разі обробки отриманого сигналу методами стиснення імпульсів, дозволяють розраховувати на забезпечення роздільної здатності цілей на дальності на рівні 10-15 см. Експериментально продемонстровано багаторазове (більш ніж на порядок) зменшення інтерференційних флуктуацій прийнятого сигналу, зумовлених фасетковою природою зворотного розсіювання цілей, у разі використання шумового зонduючого імпульсу порівняно з одноразовим - частота пульсу. Окреслено шляхи подальшої роботи з розробки та практичного застосування побудованої вимірювальної системи.

Ключові слова: шумовий радар; активно-пасивні системи; широкосмугові шумові сигнали; міліметровий діапазон; радіометри.

Руженцев Микола Вікторович – д-р техн. наук, проф., голов. наук. співроб. каф. аерокосмічних радіоелектронних систем, Національний аерокосмічний університет ім. М. Є. Жуковського "Харківський авіаційний інститут", Харків, Україна.

Грибський Олег Петрович – старш. наук. співроб., Державне підприємство "Науково-дослідний інститут "ОРІОН", Київ, Україна.

Мальцев Сергій Борисович – старш. наук. співроб., Державне підприємство "Науково-дослідний інститут "ОРІОН", Київ, Україна.

Шевчук Сергій Дмитрович – заст. нач. від. № 91, Державне підприємство "Науково-дослідний інститут "ОРІОН", Київ, Україна.

Павліков Володимир Володимирович – д-р техн. наук, старш. наук. співроб., проректор з наукової роботи, Національний аерокосмічний університет ім. М. Є. Жуковського «Харківський авіаційний інститут», Харків, Україна.

Черепнін Гліб Сергійович – асист. каф. аерокосмічних радіоелектронних систем, Національний аерокосмічний університет ім. М. Є. Жуковського "Харківський авіаційний інститут", Харків, Україна.

Жила Семен Сергійович – д-р техн. наук, проф., зав. каф. аерокосмічних радіоелектронних систем, Національний аерокосмічний університет ім. М. Є. Жуковського «Харківський авіаційний інститут», Харків, Україна.

Церне Едуард Олексійович – асист. каф. аерокосмічних радіоелектронних систем, Національний аерокосмічний університет ім. М. Є. Жуковського "Харківський авіаційний інститут", Харків, Україна.

Nikolay Ruzhentsev – D.Sc. in Radioengineering, Department of Aerospace Radio-Electronic Systems, National Aerospace University "Kharkiv Aviation Institute", Kharkiv, Ukraine,
e-mail: nvruzh@gmail.com, ORCID: 0000-0003-3023-4927.

Oleg Gribsky – S.Sc., State Enterprise "Research Institute "Orion", Kyiv, Ukraine.

Sergey Maltsev – S.Sc., State Enterprise "Research Institute "Orion", Kyiv, Ukraine.

Sergey Shevchuk – Deputy Head of Department No. 91, State Enterprise "Research Institute "Orion", Kyiv, Ukraine.

Vladimir Pavlikov – D.Sc. in Radioengineering, Vice Rector for Science, National Aerospace University "Kharkiv Aviation Institute", Kharkiv, Ukraine,
e-mail: v.pavlikov@khai.edu, ORCID: 0000-0002-6370-1758.

Gleb Cherepnin – Assistant at the Department of Aerospace Radio-Electronic Systems, National Aerospace University "Kharkiv Aviation Institute", Kharkiv, Ukraine.
e-mail: g.cherepnin@khai.edu, ORCID: 0000-0003-1245-0933.

Simeon Zhyla – D.Sc. in Radioengineering, Head of Department of Aerospace Radio-Electronic Systems, National Aerospace University "Kharkiv Aviation Institute", Kharkiv, Ukraine,
e-mail: s.zhyla@khai.edu, ORCID: 0000-0003-2989-8988.

Eduard Tserne – Assistant at the Department of Aerospace Radio-Electronic Systems, National Aerospace University "Kharkiv Aviation Institute", Kharkiv, Ukraine,
e-mail: e.tserne@khai.edu, ORCID: 0000-0003-0709-2238.